FTIR and Ab Initio Investigations of the MTBE−Water Complex

Zhuangjie Li* and Sumitpal Singh

Department of Chemistry and Biochemistry, California State University Fullerton, Fullerton, California 92834

Received: May 13, 2008; Revised Manuscript Received: July 4, 2008

The infrared spectrum of methyl *tert*-butyl ether (MTBE) in liquid water has been studied using both FTIR absorption and FTIR−ATR spectroscopy in conjunction with ab initio calculations. Compared to the liquid MTBE IR spectrum, the C−O and C−C stretching vibrational frequencies of MTBE in water are found to shift to the red and blue by up to 26 and 9 cm^{-1}, respectively. Ab initio calculations suggest that these shifts are caused by complexation of the MTBE molecule with water molecules through hydrogen bonding. Our observation of the vibrational frequency shifts in the IR spectrum of MTBE in water provides the IR spectroscopic evidence of organics−water complexes in the diluted aqueous solution. The implication of the effect of the hydrogen bond in organics−water complexation on solvation and reactivity of the organic compound in aqueous chemical processes is discussed.

Introduction

Hydrogen bonding associated with water plays an important role in chemical and biological systems due to the fact that many reactions take place in aqueous solution and that macromolecular biological systems must contain water to maintain their structure and functions.[1] Complexation of water molecules to organic compounds via hydrogen bonding constitutes an initial step of solvation that can affect the chemistry of the organics. It is therefore essential to examine the hydrogen-bonded organics−water complexes at a molecular level in order to better understand aqueous chemical processes. There have been numerous experimental and theoretical studies regarding the hydrogen-bonded organics−water complexes.[2−16] Spectroscopic studies show that when water molecules form complexes with organic compounds, the molecular properties of the water moiety are remarkably altered.[4,10−12,16] For example, the O−H stretching bands of the water molecule are found to be broadened in various organic solvents.[12] The vibrational frequency of the O−H stretching modes (ν_1 and ν_3) is also found to shift to lower frequencies (red shift) compared with their values in the gaseous phase when the water molecules form a complex with an organic compound.[4,12−14,16,17] The shifts of O−H stretching frequencies brought about by the complexation of an organic compound with water molecules are also predicted by theoretical calculations.[4,5,8,11]

While most previous studies of organics−water complexes primarily focused on the effect of hydrogen bonding on the water moiety of the complex, much less is understood regarding the effect of the hydrogen bond on the organics moiety. Nickolov et al. reported IR spectra in the C−H stretching region of 2800−3500 cm^{-1}, which is overlapping with the O−H stretching band, for 15-crown-5 and 18-crown-6 in aqueous solution.[4] The C−H stretching vibrations of the aromatic moiety of benzene−water complexes were also observed by Miyazaki et al. at around 3100 cm^{-1}.[10] Recently, He et al. studied the water complexes of *m*-aminobenzoic acid (MABA) in the electronically excited state (S_1) using two-color resonantly enhanced multiphoton ionization (REMPI) and UV−UV hole-burning spectroscopy, and they observed a blue shift of up to 50 cm^{-1} for the in-plane bending mode of the carboxyl group of MABA due to the hydrogen bond of the MABA−water complex.[7] Givan et al. reported their investigation of a 1:1 methanesulfonic acid−water complex trapped in an Ar/H_2O matrix using Fourier transform infrared spectroscopy (FTIR) and ab initio calculations, in which they observed changes of vibrational frequencies in the methanesulfonic acid when it complexed with one water molecule.[18] There has been very little information available regarding the effect of the hydrogen bond on the property of ground-state organic compounds in aqueous organics−water complexes.

Fourier transform infrared spectroscopy has been a powerful tool to study organic molecules in gaseous, liquid, and solid phases. It would be desirable to use the FTIR technique to monitor ground-state organic compounds in aqueous solutions in which water is the dominant component. However, it is a great challenge to investigate the vibrational spectroscopy for the organic moiety of the organics−water complexes in dilute solutions due to the fact that water is strongly active in the mid-infrared (mid-IR, 4000−400 cm^{-1}) region where the fingerprints of most organic compounds are located. Nevertheless, there is a spectral window (1500−700 cm^{-1}) in the mid-IR region where the absorption cross section of water is relatively small. Since many organic compounds have functional group(s) being IR active in this region, it is likely to observe IR absorption of these compounds in aqueous solution within the window, and the FTIR detections of these organics in dilute solution can be made. Recent studies show that the combination of FTIR and attenuated total reflectance[19] (FTIR−ATR) further enhances the capability of the FTIR detection.[20−25] In this paper, we report our detection of methyl *tert*-butyl ether (MTBE) in liquid water using both FTIR and FTIR−ATR spectroscopy with the aid of ab initio molecular orbital calculations. MTBE has been used as an oxygenated additive in reformulated gasoline and oxyfuels. Because it is moderately soluble in water (44 g/L at 20 °C),[26] it is readily dissolved and transported in groundwater.[27,28] Once this compound enters the drinking water system, it becomes a water contaminant that can cause nausea, nose and throat irritations, and possible carcinogenicity if inhaled or consumed.[29] From the viewpoint of chemical physics, the oxygen atom in

* To whom correspondence should be addressed. Phone: 714-278-3585. Fax: 714-626-8010. E-mail: zli@fullerton.edu.

10.1021/jp804246b CCC: $40.75
Published on Web 08/20/2008

MTBE can serve as an important contributor for hydrogen bonding, leading to the formation of the MTBE−water complex. We observe shifts of several fundamental bands of the MTBE when this molecule is mixed with water. These shifts are attributed to the hydrogen bond formed between MTBE and water molecules in light of ab initio computational results of the MTBE·$(H_2O)_n$ ($n = 0-3$) system.

Experimental Section

Both FTIR absorption and FTIR−ATR experiments are carried out using a Nicolet 4700 FTIR spectrometer (Thermo Electron Corporation). Dry air is added to the spectrometer to purge the system of moisture during the experiments. IR spectra are taken with a spectral resolution of 2 cm^{-1}. For FTIR absorption experiments, an absorption cell made of ZnSe with a path length of 25 μm (International Crystal Laboratories) is used for obtaining the FTIR spectra. For the FTIR−ATR experiments, a horizontal attenuated total reflectance (HATR) assembly (Pike Technologies) and a crystal trough plate are used. The trough plate houses an 80 mm × 10 mm × 4 mm (length × width × thickness) ZnSe crystal. With an incident angle of 40°, there are 12 reflections in the crystal. Deionized water is used as the solvent for the MTBE solution. MTBE (99%) is purchased from Acros Organics and used as received. A water background is taken prior to all sample runs to subtract out the absorption features due to the water. The absorption cell is cleaned by continuously flushing with acetone followed by flushing with the deionized water. The crystal is cleaned with acetone-saturated cotton tip applicators, rinsed with deionized water, and vacuumed briefly.

Computational Methods

All theoretical calculations were carried out using GAUSSIAN 03 program.[30] The geometries of the MTBE and MTBE−water complexes were optimized, and frequency analysis was followed using Møller−Plesset correlation energy correction truncated at second-order (MP2) in conjunction with the 6-31G(d,p) basis set (MP2/6-31G(d,p)). All geometries were optimized to better than 0.0001 Å for bond distance and 0.01° for bond angles using Schlegel's method. Single-point energy calculations were also performed using fourth-order open-shell Møller−Plesset perturbation theory including single, double, and quadruple excitations (MP4SDQ, frozen core) in conjunction with the 6-311G++(d,p) basis set using the geometries of the species optimized at the MP2/6-31G(d,p) level of theory.

Results and Discussion

A. The FTIR Spectra of MTBE in Water. In order to minimize the spectral interference from water, a specific region of the mid-IR spectrum, namely, from 1340 to 950 cm^{-1}, is chosen for the present study. Figure 1 shows the FTIR absorption and FTIR−ATR spectra for MTBE in water along with a FTIR spectrum of 99% MTBE placed at the bottom for reference purposes. The contribution of water has been subtracted from the IR spectra of the solution. The FTIR spectrum of 99% MTBE displays a distinctive absorption pattern in the spectral region of 1340−950 cm^{-1}, with five absorption bands located at 1021, 1084, 1202, 1232, and 1263 cm^{-1}, respectively.

It is interesting to observe that, in the spectra of MTBE in water taken either with the FTIR absorption cell or with the FTIR−ATR crystal trough plate, the peaks at 1084 and 1202 cm^{-1} are shifted to lower frequency (red shift) by 26 and 4 cm^{-1}, and peaks at 1232 and 1263 cm^{-1} are shifted to higher frequency (blue shift) by 10 and 6 cm^{-1} compared to the MTBE reference spectrum, respectively. These shifts are always observed at all concentrations prepared (6−44 g/L) in the present work. This observation indicates that the shifts of the absorption peaks are associated with water and that the water surrounding environment can affect the vibrational motion of the MTBE molecule. It is conceivable that the water molecules can complex with the MTBE molecule by binding to the oxygen atom, which results in a small structural change in the MTBE molecule, giving rise to the shift of these absorption peaks in the IR spectrum. However, how water molecules result in change of the MTBE molecular structure and hence its IR spectrum remains unclear.

B. Ab Initio Calculations. In order to understand the nature of the MTBE infrared absorptions and the shift of these peaks, ab initio calculations are carried out to optimize the structure of MTBE and calculate the vibrational frequencies of MTBE in both the absence and presence of water molecules. Figure 2 shows the optimized geometry for the MTBE molecule (Figure 2a) and the MTBE·$(H_2O)_n$ ($n = 1-3$) complexes (Figures 2b, 2c, and 2d) at the MP2/6-31G(d,p) level of theory. Each of these species is a minimum on the potential energy surface since all normal vibrational frequencies of the species are positive. Table 1 shows some of the calculated vibrational frequencies of MTBE along with that observed in the MTBE FTIR spectrum, and Table 2 summarizes major calculated structural parameters and frequencies associated with these parameters. It can be seen from Figure 2b that when one H_2O molecule is added to the MTBE molecule, one of the hydrogen atoms in the water molecule interacts with the oxygen atom of the MTBE molecule through hydrogen bonding (H19···O14), forming a hydrogen bond with a bond length of 1.8894 Å. This hydrogen bond tends to weaken the carbon−oxygen bonds, that is, the C2−O14 and C15−O14 bonds, of the MTBE molecule, causing an increase in the C−O bond lengths by about 0.0129 and 0.0071 Å, respectively compared to that of the bare MTBE molecule. The weakening of the C2−O14 bond in turn causes a stronger interaction between C−C atoms in the *tert*-butyl group, which leads to a decrease in C−C bond lengths by 0.0001 (C1−C2 bond), 0.0025 (C2−C7 bond), and 0.0012 Å (C2−C6 bond), respectively.

When two water molecules are added to the MTBE molecule, a complex of MTBE·$(H_2O)_2$ is formed. As indicated in Figure 2c, both water molecules use a hydrogen atom to form hydrogen bonds with the MTBE molecule, with bond lengths of 1.9426 (H22···O14) and 2.1351 Å (H19···O14), respectively. Another hydrogen bond (O23···H21), with a bond length of 2.1054 Å, is predicted to be formed between the second hydrogen of the first water molecule with the oxygen of the second water molecule. Our computational results also predict that the C2−O14 and C15−O14 bond lengths of the MTBE moiety in the MTBE·$(H_2O)_2$ complex further increase by 0.0050 and 0.0031 Å, respectively, and the C1−C2, C2−C6, and C2−C7 bond lengths are anticipated to further decrease by 0.0001, 0.0011, and 0.0010 Å, respectively, compared with those in the MTBE·(H_2O) complex (Table 2). This indicates that the additional hydrogen bonding further alters the structure of MTBE in a way of intensifying the changes caused by the first hydrogen bond.

On the basis of our computational results, the addition of a third water molecule to the MTBE·$(H_2O)_2$ complex does not increase the number of hydrogen bonds between MTBE and water molecules. As shown in Figure 2d, only two water molecules interact with the MTBE molecule through hydrogen bonds with bond lengths of 2.0512 (H22···O14) and 1.8533 Å

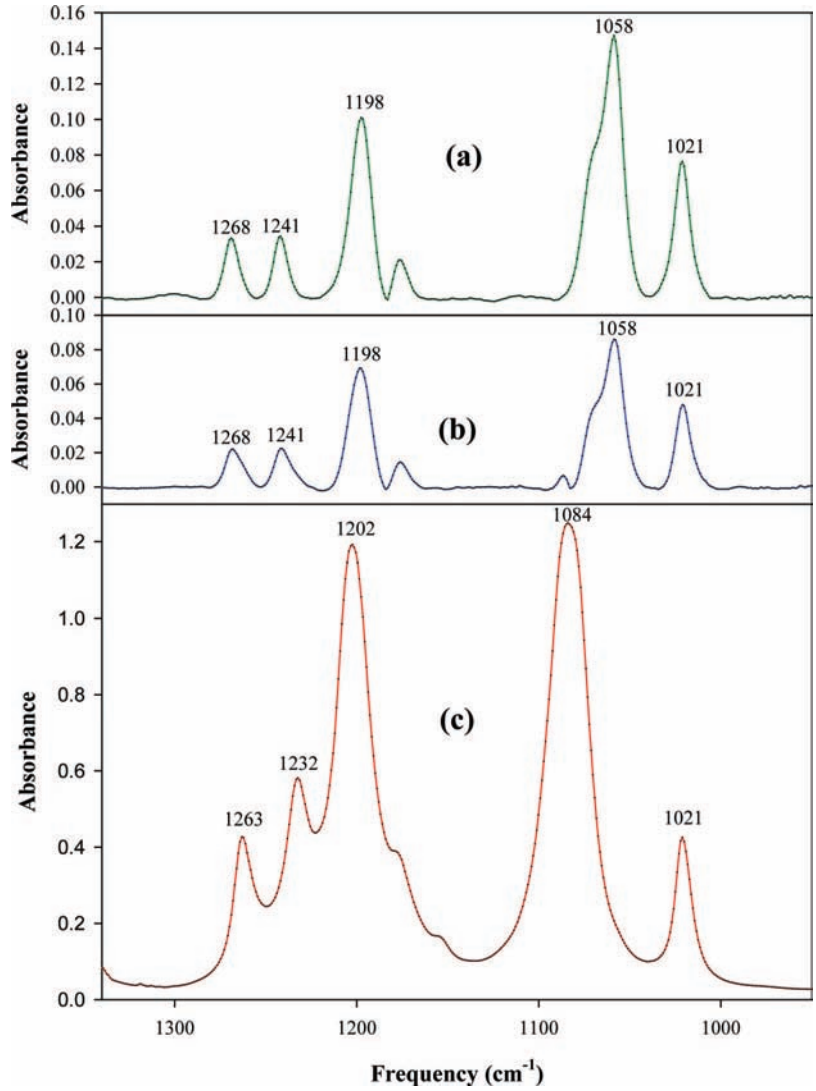

Figure 1. Infrared spectra of MTBE in water (a and b) and liquid MTBE (c) with labeled frequencies in cm^{-1}. The spectra (a) and (b) are taken using a 25 μm absorption cell and an attenuated total reflection (ATR) trough plate, respectively. The concentration of the MTBE solution is 44 g/L. The contribution of water has been subtracted from the IR spectra of the solution. The spectrum (c) was obtained using the ATR trough plate.

(H25···O14), respectively. The third water molecule joins the complex by connecting its oxygen and the second hydrogen to the other two water molecules that are attached to MTBE, and the resulting hydrogen bond lengths are calculated to be 1.9441 (H24···O20) and 1.8503 Å (H19···O26), respectively. This type of complexation further increases the C−O bond lengths of the MTBE moiety by ∼0.0063 (C2−O14) and ∼0.0012 Å (C15−O14) compared with that of the MTBE·$(H_2O)_2$ complex. The addition of a third water molecule also causes small decreases of about 0.0001 and 0.0018 Å in the C1−C2 and C2−C6 bond lengths, respectively. However, the C2−C7 bond is predicted to increase by 0.0008 Å compared with that of the MTBE·$(H_2O)_2$ complex.

In the present study it is important to consider the solvent effect on the molecular structure and vibrations of the MTBE through electrostatic interaction since water has a high dielectric constant. Therefore, an additional calculation on MTBE was performed using the polarizable continuum model[31] (PCM) to assess the significance of this solvation effect, and the results are given in Table 2. The structure of MTBE is predicted to change slightly by the electrostatic interaction, with increases of 0.0035 and 0.0049 Å in the C15−O14 and C2−O14 bonds and a decrease of 0.0002 Å in the C6−C7 bond, respectively. The C1−C2 bond is essentially unchanged. Compared to the MTBE·$(H_2O)_n$ complexes, the structural changes brought about by the electrostatic interaction appear to be minor ones.

Our calculation results reveal several interesting features regarding the MTBE·$(H_2O)_n$ (n = 1−3) complex. First, the MTBE forms a complex with water molecules through hydrogen bonds. Second, the MTBE can directly complex to a maximum of two water molecules through hydrogen bonds. Third, the hydrogen bonds bridging water molecules and MTBE may vary in bond length. Finally, the backbone structure of the MTBE molecule experiences changes when the MTBE molecule forms complexes with water molecules through hydrogen bonds. The changes include an increase in the C−O bond lengths and a decrease in the C−C bond lengths.

C. Interpretation of Experimental Observation. The calculated IR spectrum of MTBE can be used to interpret the experimental IR spectrum of the MTBE. Figure 3 shows the calculated and the experimental IR spectra of MTBE. It is expected that the computed frequencies are usually higher than that experimentally observed since it is well-known that the computed force constants are always systematically larger.[2,5,7,17,32]

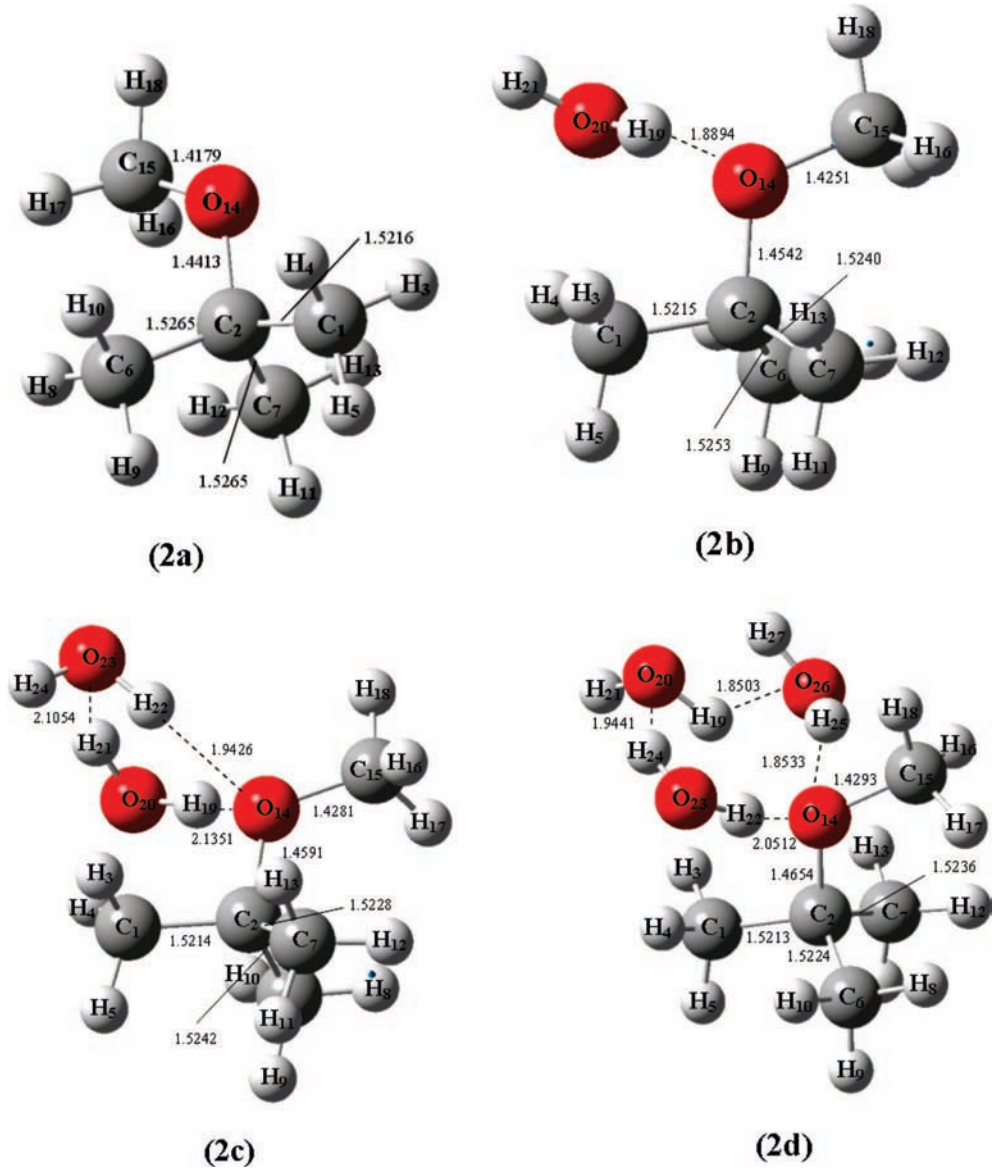

Figure 2. Optimized structure of MTBE (2a), MTBE·(H_2O) (2b), MTBE·(H_2O)$_2$ (2c), and MTBE·(H_2O)$_3$ (2d). The optimization is carried out at the MP2/6-31G(d,p) level of theory. The bond lengths displayed are in Å.

TABLE 1: Comparison of the Calculated Vibrational Frequencies (cm^{-1}) of MTBE with the Experimental Values[a]

υ[b]	mode description[c]	calculated	calc. int. (KM/mol)	expl.	expl int. (relative)
12	C_2-C_6 symmetric stretch	750	5.2	724	51
13	C_2-O_{14} stretch (symmetric)	898	14.1	851	79
18	CH_3 rock	1074	2.8	1021	30
19	$C_{15}-O_{14}$ stretch (carbon on methyl group)	1150	84.8	1084	100
22	C_2-O_{14} stretch (tertiary carbon, asymmetric)	1282	93.9	1202	95
23	C_2-C_7 stretch (tertiary carbon, asymmetric)	1310	16.7	1232	41
24	C_1-C_2 stretch (asymmetric tertiary carbon)	1337	16.6	1263	35
25	CH_3 umbrella	1441	15.9	1364	76
27	CH_3 umbrella	1468	8.5	1385	37
32	CH_2 scissoring	1552	3.4	1436	7
36	$H_8-C_6-H_{10}$ bending	1580	10.8	1469	28
37	symmetric $C_{15}-H_{16}$ stretch (methyl group)	3097	43	2827	23
39	C_1-H_4 stretch, symmetric	3127	20.2	2905	31
41	asymmetric $C_{15}-H_{16}$ stretch (methyl group)	3175	57.3	2940	41
48	C_1-H_5 stretch, asymmetric	3236	24.8	2974	83

[a] The frequencies are calculated following the geometry optimization at the MP2/6-31G(d,p) level of theory, and the frequencies are not scaled. The experimental values are based on the IR spectrum obtained in the present work. [b] Mode numbers are assigned based on the computational results. [c] Referred to Figure 2 for numbering of the atoms of the MTBE molecule.

On the basis of comparison of the fundamental frequencies and relative intensity of the calculated IR spectrum with those of the experimental IR spectrum, the observed vibrational peaks at 1084 and 1202 cm^{-1} are assigned to C−O stretching between

TABLE 2: Calculated Major Bond Lengths and Vibrational Frequencies of MTBE·$(H_2O)_n$ ($n = 0-3$)[a]

	species	$\nu_{C15-O14}$[b] / *$r_{C15-O14}$*[b]	Δ[c]	ν_{C2-O14}[b] / *r_{C2-O14}*[b]	Δ[c]	ν_{C-C}[b] / r_{C2-C7}[b] / *r_{C2-C6}*[b]	Δ[c]	ν_{C1-C2}[b] / *r_{C1-C2}*[b]	Δ[c]
calc.	MTBE	1150		1282		1310		1337	
		1.4179		*1.4413*		*1.5265*		*1.5216*	
						1.5265			
	MTBE·(H_2O)	1136	−14	1273	−9	1318	+8	1341	+4
		1.4251	*0.0071*	*1.4542*	*0.0129*	*1.5240*	*−0.0025*	*1.5215*	*−0.0001*
						1.5253	*−0.0012*		
	MTBE· $(H_2O)_2$	1130	−20	1268	−14	1320	+10	1343	+6
		1.4281	*0.0102*	*1.4591*	*0.0178*	*1.5228*	*−0.0036*	*1.5214*	*−0.0002*
						1.5242	*−0.0022*		
	MTBE· $(H_2O)_3$	1127	−23	1266	−16	1323	+13	1343	+6
		1.4293	*0.0114*	*1.4654*	*0.0241*	*1.5236*	*−0.0028*	*1.5213*	*−0.0003*
						1.5224	*−0.004*		
	MTBE + solvent effect[d]	1134	−16	1271	−11	1308	−2	1335	−2
		1.4232	*0.0035*	*1.4462*	*0.0049*	*1.5263*	*−0.0002*	*1.5216*	*0.0000*
						1.5263	*−0.0002*		
expl.	MTBE	1084		1202		1232		1263	
	MTBE in water	1058	−26	1198	−4	1241	+9	1268	+5

[a] Calculations are carried out at the MP2/6-31G(d,p) level of theory. Frequencies are in cm^{-1}. The italic values are bond lengths in Å. [b] $\nu_{C15-O14}$ and $r_{C15-O14}$ stand for the C15−O14 stretching and bond length, ν_{C2-O14} and r_{C2-O14} stand for the C2−O14 stretching and bond length, ν_{C1-C2} and r_{C1-C2} stand for the C1−C2 stretching and bond length, and ν_{C-C}, r_{C2-O7}, and r_{C2-O6} stand for C−C stretching and C2−C7 and C2−C6 bond lengths, respectively. [c] Δ stands for the difference in the vibrational frequency and bond length reference to bare MTBE. [d] Calculation is carried out at the MP2/6-31G(d,p) level of theory taking into account solvent effects using the polarizable continuum model (PCM).

an oxygen atom and a carbon atom on the methyl group (C15−O14) and between the oxygen atom and the tertiary carbon (C2−O14), respectively. Whereas, the peak at 1232 cm^{-1} is assigned to C2−C6/C2−C7 stretching, and the peak at 1263 cm^{-1} is assigned to C1−C2 stretching. The assignment of the peak at 1232 cm^{-1} to both C2−C6/C2−C7 stretching is preferred because they are strongly coupled and essentially inseparable. The calculated and experimental frequencies of MTBE in the IR range of 1350−950 cm^{-1} are given in Table 2 for comparison. It can be seen that the calculated frequencies of MTBE are in good agreement with the experimental frequencies, with overestimates up to 7.2%.

The structural changes of the MTBE brought about by the hydrogen bonding due to complexing with water molecules are expected to result in a shift in vibrational frequencies for corresponding stretching modes. As shown in Table 2, when 1, 2, and 3 water molecules are added to MTBE, the frequency of the C15−O14 stretching mode is predicted to shift to the red by 14, 20, and 23 cm^{-1}, and the frequency of C2−O14 stretching mode is expected to shift to the red by 9, 14, and 16 cm^{-1}, respectively. Meanwhile, the frequency of the C−C stretching modes is predicted to shift to the blue by 8, 10, and 13 cm^{-1} for C2−C7/C2−C6 stretching and 4, 6, and 6 cm^{-1} for C1−C2 stretching, respectively. The shifts observed from our IR spectra of MTBE dissolved in water (see Figure 1 and Table 2) are 26 and 4 cm^{-1} to the red for the C15−O14 and C2−O14 stretching modes and 10 and 6 cm^{-1} to the blue for the C2−C7/C2−C6 and C1−C2 stretching modes compared to the bare MTBE FTIR spectrum, respectively. Note that the peak at 1021 cm^{-1}, assigned to the CH_3 rocking vibration, is not changed after the MTBE is dissolved in water, indicating that the hydrogen bonds have little effect on the vibrations that are not associated with the backbone of the MTBE molecule. Thus, our computation results capture the features of the vibrational frequency shift of the MTBE molecule under the influence of hydrogen bonds, although the absolute values of the shifts are not all matched. Similar red and blue shifts of vibrational frequencies of organics due to the complex with water hydrogen bonding have been observed in the 1:1 $CH_3SO_2OH·H_2O$ complex trapped in an Ar matrix, in which the S−O and C−S stretching modes are shifted to the blue by up to 51.6 cm^{-1} and the SO_2 antisymmetric symmetric stretching modes to the red by up to 89.4 cm^{-1} compared to that of the monomeric CH_3SO_2OH on an Ar matrix.[18] This observation supports our understanding of vibrational frequency shift in the FTIR and FTIR−ATR spectra of the MTBE·$(H_2O)_n$ complex. Finally, our PCM calculation on the MTBE molecule predicts that the vibrational frequencies associated with these bonds shift to red by 2−16 cm^{-1}, which is in contrast to both the hydrogen bonding effect on the MTBE vibrations and the experimental observations. This suggests that the prediction of the frequency shifts using the PCM model may not be accurate for the MTBE molecule.

D. The Energetics of the MTBE−Water Complex. Table 3 shows the calculated total energy and relative energy for the complex reaction of MTBE with 1−3 water molecules,

$$\text{MTBE} + n\text{H}_2\text{O} \rightarrow \text{MTBE}\cdot(\text{H}_2\text{O})_n \qquad (n = 1-3) \quad (1)$$

Our computational data indicated that at the MP2/6-31G(d,p) level of theory, the MTBE complexation with water is predicted to be exothermic by 9.5, 19.0, and 31.9 kcal mol^{-1} when the MTBE complexes to 1, 2, and 3 water molecules, respectively. The exothermicity is significantly reduced to 2.4, 3.2, and 8.7 kcal mol^{-1} at the MP4SDQ/6-311++G(d,p) level of theory, suggesting that the higher-order perturbation and larger basis set are important in the determination of the energetic property of this chemical system. Inclusion of the zero-point energy correction results in the best estimated reaction enthalpies of −0.03, +1.7, and −1.0 kcal mol^{-1} for $n = 1$, 2, and 3, respectively. This suggests that the MTBE−water complex may not be thermodynamically favored for $n = 1$ and 2, but MTBE·$(H_2O)_n$ is expected to be formed when $n \geq 3$ due to the increase of hydrogen bonding in the system. In the case of MTBE dissolving in water, many more water molecules are available for complexation and clustering with the MTBE molecule, making

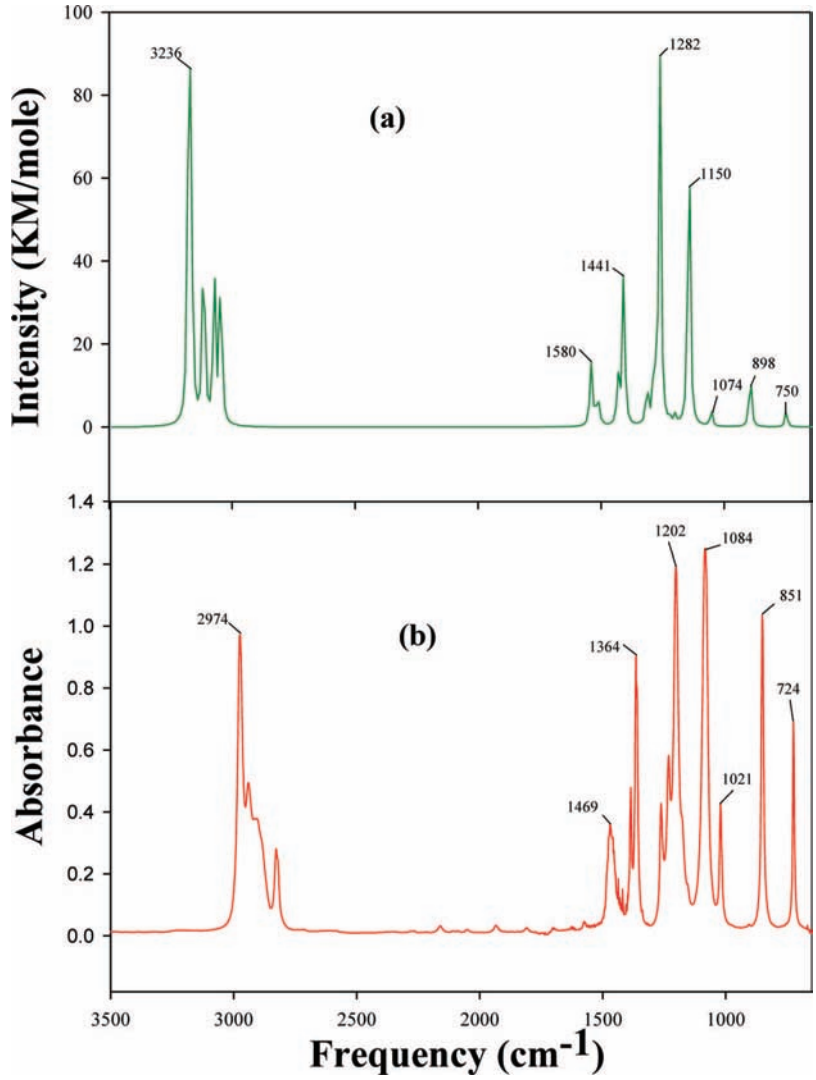

Figure 3. Comparison of the calculated IR spectrum without scaling (a) and the experimental IR spectrum (b) of MTBE. The calculated IR spectrum is generated from the frequency computation of the optimized MTBE molecule at the MP2/6-31G(d,p) level of theory using a width of 10 cm^{-1} for the half-width at half-height. The experimental IR spectrum of MTBE is obtained using the ATR trough plate.

TABLE 3: Calculated Total Energy (in Hartree) and Relative Energy (in kcal mol^{-1}) of the MTBE + $nH_2O \rightarrow$ MTBE·$(H_2O)_n$ ($n = 1-3$) System

total energy	MP2/6-31G(d,p)	zero-point energy (Z.P.E.)	MP4SDQ/6-311++G(d,p)	MP4SDQ/6-311++G(d,p) + Z.P.E.
MTBE	−272.11270	0.16912	−272.29747	−272.12835
H_2O	−76.21979	0.02189	−76.29484	−76.27295
MTBE·(H_2O)	−348.34721	0.19480	−348.59615	−348.40135
MTBE·$(H_2O)_2$	−424.58219	0.22066	−424.89227	−424.67161
MTBE·$(H_2O)_3$	−500.82253	0.24719	−501.19588	−500.94869
		relative energy		
MTBE + $H_2O \rightarrow$ MTBE·(H_2O)	−9.5	2.4	−2.4	−0.03
MTBE + $2H_2O \rightarrow$ MTBE·$(H_2O)_2$	−19.0	4.9	−3.2	1.7
MTBE + $3H_2O \rightarrow$ MTBE·$(H_2O)_3$	−31.9	7.7	−8.7	−1.0

the MTBE·$(H_2O)_n$ complex thermodynamically stable. This has led to the observation of the peak-shifted IR spectrum of MTBE in water, as shown in Figure 1.

E. Implications of Aqueous MTBE−Water Complexation. There are several implications in the present findings of the hydrogen-bonding effect on the MTBE moiety of the MTBE·$(H_2O)_n$ complex. The shifts of vibrational frequencies suggest that if an organics−water complex forms through hydrogen bonding, the IR spectral identification of the organics in dilute aqueous solution may be different from that of pure compound due to the change of locations of some fingerprints. Furthermore, an organic compound can only interact with a limited number of water molecules directly through hydrogen bonds, and in the case of MTBE, the number is two. It is the complexation of the organic compound with the water molecule that initiates the solvation of the organics in water. In addition, the complexation of the organic compound with water causes structural alteration of the organic compound, and this could play a role in changing the reactivity of the organics in the solution since the increase of the bond length owing to the presence of the hydrogen bond may weaken that chemical bond. It is likely that the activation energy can be lowered to break

certain bonds in an organic compound that are weakened because of the hydrogen bond formed in the complex, which will increase the reaction rate of an aqueous chemical process. The hydrogen bond between the organics and water may therefore open a door for further insight of chemical processes in the aqueous phase.

Conclusion

The present study has investigated the infrared spectrum of MTBE in water using both FTIR absorption and FTIR−ATR spectroscopy. The peaks at 1058, 1198, 1241, and 1268 cm^{-1} in the IR spectra of the MTBE−water aqueous solution are the result of the shifts of vibrational frequencies of the MTBE molecule due to its complexing to water molecules. Ab initio calculations lead to the assignment of these peaks to C−O (1058 and 1198 cm^{-1}) and C−C (1241 and 1268 cm^{-1}) stretching of the MTBE molecule. The experimental observation of the red shift of the C−O bond and the blue shift of the C−C bond agrees with the theoretical calculation results for the MTBE·$(H_2O)_n$ ($n = 1-3$) complexes, in which the MTBE interacts with the water molecule through hydrogen bonds. While the organic−water complexes have been observed in ice surfaces at low temperatures, our observation of the vibrational frequency shifts in the IR spectrum of MTBE in water provides the IR spectroscopic evidence of an organics−water complex in dilute aqueous solution. The fact that the IR frequencies shift indicates a structural change of the MTBE molecule upon complexation with water molecules via hydrogen bonding. The change of the organic structure due to forming a complex with water may play a role in the solvation of the organic compound and the reactivity of the organics in aqueous chemical processes.

Acknowledgment. This work was supported, in part, by the National Science Foundation (NSF ATM-0533574), the CSU Special Fund for Research, Scholarship, and Creative Activity Minigrant, and the Untenured Faculty Support Grants of CSUF.

References and Notes

(1) Jeffrey, G. A. *An Introduction to Hydrogen Bonding*; Oxford University Press, Inc.: New York, 1997.
(2) Rablen, P. R.; Lockman, J. W.; Jorgensen, W. L. *J. Phys. Chem. A* **1998**, *102*, 3782–3797.
(3) Li, Y.; Liu, X.-H.; Wang, X. Y.; Lou, N.-Q. *J. Phys. Chem. A* **1999**, *103*, 2572–2579.
(4) Nickolov, Z. S.; Ohno, K.; Matsuura, H. *J. Phys. Chem. A* **1999**, *103*, 7544–7551.
(5) Fredericks, S. Y.; Jordan, K. D. *J. Phys. Chem.* **1996**, *100*, 7810–7821.
(6) Bryan, S. A.; Willis, R. R.; Moyer, B. A. *J. Phys. Chem.* **1990**, *94*, 5230–5233.
(7) He, Y.; Wu, C.; Kon, W. *J. Phys. Chem. A* **2005**, *109*, 748–753.
(8) Wang, L. *J. Phys. Chem. A* **2007**, *111*, 3642–3651.
(9) Han, J.; Deming, R. L.; Tao, F.-M. *J. Phys. Chem. A* **2005**, *109*, 1159–1167.
(10) Miyazaki, M.; Fujii, A.; Ebata, T.; Mikami, N. *J. Phys. Chem. A* **2004**, *108*, 10656–10660.
(11) Iwamoto, R.; Matsuda, T.; Sasaki, T. *J. Phys. Chem. B* **2003**, *107*, 7976–7980.
(12) Conrad, M. P.; Strauss, H. L. *J. Phys. Chem.* **1987**, *91*, 1668–1673.
(13) Garrett, A. W.; Zwier, T. S.; Severance, D. L. *J. Phys. Chem.* **1992**, *96*, 9710–9718.
(14) Suzuki, S.; Green, P. G.; Bumgarner, R. E.; Dasgupta, S.; Oddard, W. A.; Blake, G. A. *Science* **1992**, *257*, 942–945.
(15) Tanabe, S.; Ebata, T.; Fujii, M.; Mikami, N. *Chem. Phys. Lett.* **1993**, *215*, 347–352.
(16) Besnard, M.; Danten, Y.; Tassaing, T. *J. Chem. Phys.* **2000**, *113*, 3741–3748.
(17) Allen, H. C.; Raymond, E. A.; Richmond, G. L. *J. Phys. Chem. A* **2001**, *105*, 1649–1655.
(18) Givan, A.; Loewenschussa, A.; Nielsen, C. J. *J. Mol. Struct.* **2005**, *748*, 77–90.
(19) Harris, D. C. *Quantitative Chemical Analysis*, 7th ed.; W. H. Freeman: New York, 2007.
(20) Roy, G.; Mielczarski, J. A. *Water Res.* **2002**, *36*, 1902–1908.
(21) Murphy, B.; McLoughlin, P. *Int. J. Environ. Anal. Chem.* **2003**, *83*, 653–662.
(22) Karlowatz, M.; Kraft, M.; Mizaikoff, B. *Anal. Chem.* **2004**, *76*, 2643–2648.
(23) Regan, F.; Meaney, M.; Vos, J. G.; MacCraith, B. D.; Walsh, J. E. *Anal. Chim. Acta* **1996**, *334*, 85–92.
(24) Colume, A.; Diewok, J.; Lendl, B. *Int. J. Environ. Anal. Chem.* **2004**, *84*, 835–844.
(25) Jelev, A.; Ciobanu, M. F.; Frunza, L. *Chem. Pap.* **1999**, *53*, 98–101.
(26) Lide, D. R. *Handbook of Chemistry and Physics*, 87th ed.; CRC Press: Boca Raton, FL, 2006−2007.
(27) Squillace, P. J.; Zogorski, J. S.; Wilber, W. G.; Price, C. V. *Environ. Sci. Technol.* **1996**, *30*, 1721.
(28) Michalkova, A.; Johnson, L. D.; Gorb, L.; Zhikol, O. A.; Shishkin, O. V.; Leszczynski, J. *Int. J. Quantum Chem.* **2005**, *105*, 325.
(29) *CCL 1 List and Regulatory Determinations*; U.S. Environmental Agency: Washington, DC, 1998.
(30) Frisch, M. J. Trucks, G. W.; Schlegel, H. B.; Scuseria, G. E.; Robb, M. A.; Cheeseman, J. R.; Montgomery, J. A., Jr.; Vreven, T.; Kudin, K. N.; Burant, J. C.; Millam, J. M.; Iyengar, S. S.; Tomasi, J.; Barone, V.; Mennucci, B.; Cossi, M.; Scalmani, G.; Rega, N.; Petersson, G. A.; Nakatsuji, H.; Hada, M.; Ehara, M.; Toyota, K.; Fukuda, R.; Hasegawa, J.; Ishida, M.; Nakajima, T.; Honda, Y.; Kitao, O.; Nakai, H.; Klene, M.; Li, X.; Knox, J. E.; Hratchian, H. P.; Cross, J. B.; Bakken, V.; Adamo, C.; Jaramillo, J.; Gomperts, R.; Stratmann, R. E.; Yazyev, O.; Austin, A. J.; Cammi, R.; Pomelli, C.; Ochterski, J. W.; Ayala, P. Y.; Morokuma, K.; Voth, G. A.; Salvador, P.; Dannenberg, J. J.; Zakrzewski, V. G.; Dapprich, S.; Daniels, A. D.; Strain, M. C.; Farkas, O.; Malick, D. K.; Rabuck, A. D.; Raghavachari, K.; Foresman, J. B.; Ortiz, J. V.; Cui, Q.; Baboul, A. G.; Clifford, S.; Cioslowski, J.; Stefanov, B. B.; Liu, G.; Liashenko, A.; Piskorz, P.; Komaromi, I.; Martin, R. L.; Fox, D. J.; Keith, T.; Al-Laham, M. A.; Peng, C. Y.; Nanayakkara, A.; Challacombe, M.; Gill, P. M. W.; Johnson, B.; Chen, W.; Wong, M. W.; Gonzalez, C.; Pople, J. A. *Gaussian 03*; Gaussian, Inc.: Wallingford, CT, 2004.
(31) Miertuš, S.; Scrocco, E.; Tomasi, J. *Chem. Phys.* **1981**, *55*, 117–129.
(32) Johnson, B. G.; Gill, P. M. W.; Pople, J. A. *J. Chem. Phys.* **1993**, *98*, 5612–5626.

JP804246B